Field Weakening Design for a High Speed Nine-phase Permanent Magnet Synchronous Machine in More Electric Aircraft

Mi Tang
Power Electronics, Machine and Control Group
University of Nottingham
Nottingham, UK
mi.tang@nottingham.ac.uk

Yuzheng Chen
Power Electronics, Machine and Control Group
University of Nottingham
Nottingham, UK
yuzheng.chen@nottingham.ac.uk

Tao Yang
Power Electronics, Machine and Control Group
University of Nottingham
Nottingham, UK
tao.yang@nottingham.ac.uk

Abstract—**High speed multi-phase permanent magnet synchronous machine (PMSM) offers increased power density and fault-tolerant ability, which qualifies it a promising solution for the ever-increasing power and reliability demands of more electric aircraft (MEA). Pushed by the high-speed design, high performance field weakening control of the machine necessarily demanded. Under the concept of field oriented control (FOC), field weakening methods can be designed considering different priority between d and q axis control. This paper aims comparing those differences and proposing the suitable solution for the high speed PMSM drive in MEA. The equivalent circuit of the field weakening loop is derived, which demonstrates the tuning of the field weakening controller in terms of stability and performance without considering the anti-windup and saturations. Recommendations on the design of anti-windup and saturations considering d and q-axis prioritizations are provided.**

I. Introduction

In recent years a significant progress has been made towards more electric aircraft (MEA) in the aerospace industry. The MEA concept brings different advantages including a higher efficiency, favourable environmental impacts, decreased fuel consumption, and lower maintenance costs compared with conventional solutions [1]. In the paradigm of MEA, many onboard components and systems conventionally driven by the hydraulic or pneumatic powers, are replaced by their electrical counterparts. Consequently, a sufficient electrical power generation capability is required.

In an aircraft, the engine performs as the prime power source. Due to the relatively high and constant speed of the high-pressure spool (HPS) of the engine, typically an electrical generator is driven by the HPS because the high-speed characteristic enables the size and weight reduction of the generator at a given power rating [2]. For a considered high-speed PMSM based generator, the high operation speed of the generator indicates a significant back EMF [2]. However, considering the limited DC voltage as per the aerospace standard [3], the high back EMF must be restricted for not violating the limitation of DC bus voltage. In this case, the field-weakening (FW) technique becomes a necessity.

For the application of the high-speed PMSM drive, the key factors that differ FW methods from each other are how the dq-axis currents are distributed and how the dq-axis voltages are saturated. Popular methods for calculating the dq-axis current references includes the angle advanced method [4], [5] and the lookup table with minimum flux per torque (MFPT) method [6], [7]. For the angle advanced method, it uses an outer voltage loop to automatically identify the onset of the FW control and generate a negative d-axis current to prevent the saturation of current controllers at the high-speed range (i.e., beyond the base speed of the generator). For the MFPT mthod, the general idea is to create two 3-D tables based on machine parameters and DC bus voltages, where the machine's flux serves as the searching index.

To avoid the angle computation in the first method and the flux estimator in the second method, a resemble of the angle advanced method is proposed in this paper. The equivalent circuit of the FW loop is derived and parameter tuning of the FW controller is presented in terms of stability and performance. Recommendations on the design of anti-windup and saturations considering d and q-axis prioritizations are also provided in this paper.

II. Field Weakening Loop Design

A high speed nine-phase PMSM has been designed for MEA, where, to maximize its fault-tolerant ability, the nine-phase machine can be understood as three three-phase machines sharing the same rotor and shaft. The magnetic interaction between the three triple phases is negligible. Therefore, each three-phase can be controlled independently. The machine parameters is got from FEA simulation and shown in Table I. The fundamental frequency of the machine is up to 2 kHz.

TABLE I. Machine and Control Parameters

Item	Value	Item	Value
Number of pole pairs Pp	6	Magnetic flux Fm [wb]	0.0276
Stator resistance Rs per phase [Ohms]	0.1331	Rated current (peak) Irated [A]	57.8272
DQ-axis inductance Ld=Lq=Ls per sector [H]	5.271e-4	Maximum speed [rpm]	20k
Base speed ωbase [rpm]	12k	Maximum current (peak) Imax [A]	(1.5-2) Irated
DC bus voltage Vdc [V]	540	Rated power P [kW]	50
Sampling period Ts [s]	1/fs	Sampling & switching frequency fs [Hz]	40 kHz

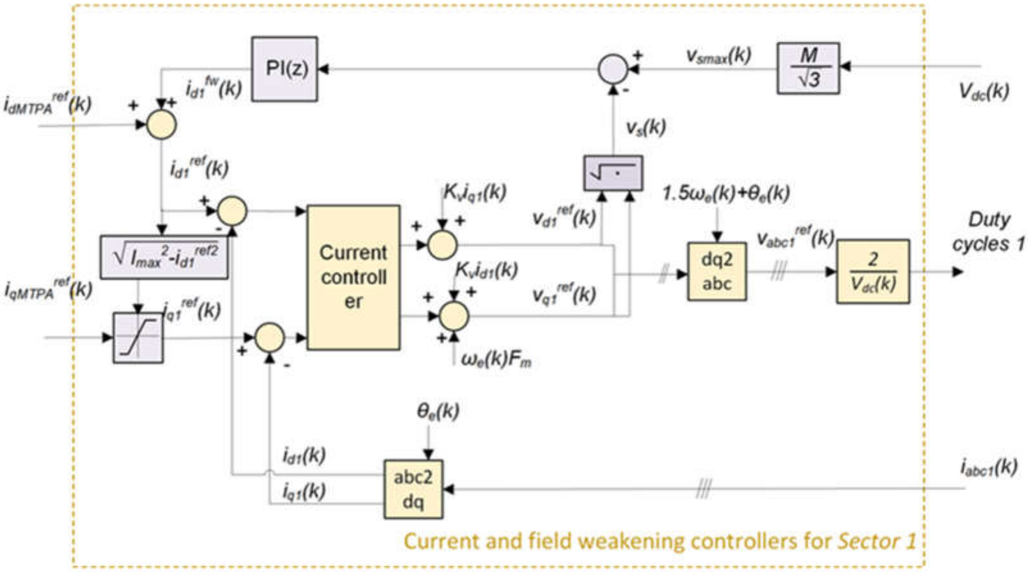

(a) Field weakening loop without anti-windup and staturations

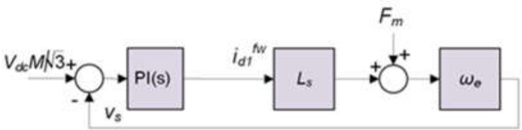

(b) Linearized equivalent diagram of (a)

Fig.1 Field weakening loop and its equivalent diagram.

Fig.1(a) is drawn for one three-phase sector of the nine-phase machine. Where, i_d and i_q are the dq-axis currents, respectively. v_d and v_q are the dq-axis voltages, respectively. "1" denotes for sector 1. "ref" denotes the reference, "MTPA" denotes maximum torque per amp, "fw" denotes field weakening, "k" denotes the k^{th} period. $K_v=\omega_e L_s$, ω_e is the electrical angular frequency, θ_e is the electrical angle, F_m is the magnetic flux. V_{dc} is the dc bus voltage, I_{max} is the maximum stator current. v_{smax} is the maximum stator voltage. PI denotes the proportional-integral controller. Moreover, the permanent magnet is surface mounted, so, the dq-axis inductances are considered equal. Hence, $i_{dMTPA}^{ref}=0$. M is the maximum achievable modulation index, typically between zero and one. $M=1$ is set in this paper.

The field weakening loop can be designed step-by-step in the following subsections:

A. *Tuning of the PI considering stability*

The PI in the field weakening loop can be tuned without considering the anti-windup and saturations. It can also be designed in s-domain and then discretized for digital implementation. As shown in Fig.1(a), the relationship between the amplitude of stator voltage v_s and d-axis current i_{d1} is not linear. The equation is given in (1).

$$\left(\frac{v_s}{\omega_e L_s}\right)^2 = \left(i_{d1} + \frac{F_m}{L_s}\right)^2 + i_{q1}^2$$
$$\Longrightarrow \frac{v_s}{\omega_e L_s} = \left[i_{d1}^2 + 2 i_{d1}\frac{F_m}{L_s} + \frac{F_m{}^2}{L_s{}^2} + i_{q1}^2\right]^{0.5} \quad (1)$$

Assumption 1: the dynamic of the field weakening loop is far slower than the current loop.

Following Assumption 1, i_{q1} can be considered as a constant and independant from i_{d1}, which does not affect the dynamic of v_s. Therefore, the relationship between i_{d1} and v_s can be simplifed as in (2).

$$\frac{\partial v_s/\omega_e L_s}{\partial i_{d1}} = 0.5 * 2 i_{d1} + 0.5 * 2 * \frac{F_m}{L_s} = i_{d1} + \frac{F_m}{L_s}$$
$$\Longrightarrow \frac{\partial v_s}{\partial i_{d1}} = \omega_e (L_s i_{d1} + F_m) \quad (2)$$

Therefore, the plant for the field weakening loop is linearized as in (2). Its equivalent diagram is illustrated in Fig.1(b). The closed loop transfer function of the field weakening loop is as in (3).

$$G_{fw}(s) = \frac{L_s\omega_e(K_{fwp}s + K_{fwi})}{(1 + L_s\omega_e K_{fwp})s + L_s\omega_e K_{fwi}}$$
$$\overrightarrow{K_{fwp} = 0}\ G_{fw}(s) = \frac{L_s\omega_e K_{fwi}}{s + L_s\omega_e K_{fwi}} \quad (3)$$

Where, K_{fwp} and K_{fwi} are the proportional and integral gains of the PI, respectively. When $K_{fwp}=0$, the closed loop is further simplied as a first order system.

Since the closed loop pole in (3) varies with rotor speed. To fix the dynamic of the field weakening loop, K_{fwi} needs to be updated online with the rotor speed. Alternatively, K_{fwi} can be fixed and *Assumption 1* should hold considering the minimum and maximum speed in field weakening opertion.

The line-line peak value of the Back-EMF provided by the machine designer is 389.1V at the base speed of 12 krpm. With full torque, the line-line peak voltage of each Sector at steady state will be close to the dc-link voltage 540V. So, the speed range where field weakening is required in this project is roughly between 12 krpm to 20 krpm. The closed loop Bode plots of the field weakening loop at 12 krpm and 20 krpm are shown in Fig.2 with $K_{fwp}=0$, $K_{fwi}=10$. As shown, the bandwidth of the field weakening loop is between 5.3 to 8.8 Hz, while the curernt loop bandwidth is designed to 700~1000 Hz.

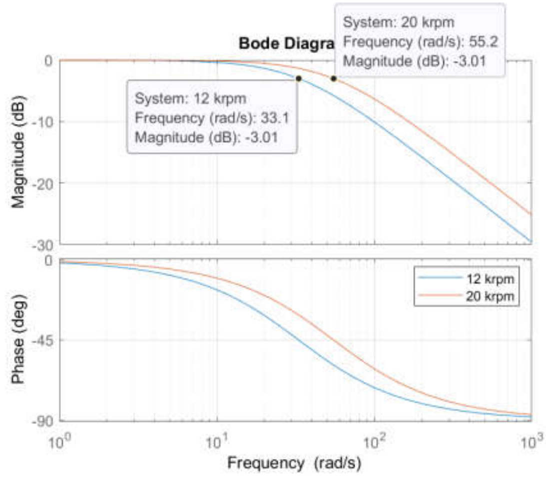

Fig.2 Closed loop Bode plot of the field weakening loop.

B. Design the anti-windup and saturation schemes

Anti-windup is necessarily used in controllers to limit the value at the output of an integrator. Popular anti-windup schemes include clamping and back-calculation [8]. Saturation is also naturally included in the modulation, since the duty cycle of any switch is always within zero to one. In this paper, the anti-windup scheme chosen for the field weakening PI is clamping. Saturation is necessary to limit the value of the voltage reference. A back-calculation based anti-windup scheme combined with saturation of v_s is proposed in [9], which improves the dc voltage usage.

However, the method in [9] only considers equal prioritization between d and q axis. In fact, the saturation scheme varies with the choice of d-axis prioritization, q-axis prioritization, and equal prioritization. This paper adds the possibility of choosing prioritization to the method in [9] and compares the three choices. Overall, the proposed field weakening loop with anti-windup and saturations are drawn in Fig.3.

Let $v_{max} = V_{dc}/\sqrt{3}$:

1) If d-axis has the priority, then (4) is hold:

$$\begin{aligned} v_{d1}^{sat} &= min(max(v_{d1}^{ref},\ -v_{max}), v_{max}) \\ v_{q1}^{sat} &= min(max(v_{q1}^{ref}, -v_{max}), v_{max2}) \end{aligned} \tag{4}$$

where, $v_{max2} = \sqrt{v_{max}^2 - {v_{d1}^{ref}}^2}$.

2) If q-axis has the priority, then (5) is hold:

$$\begin{aligned} v_{q1}^{sat} &= min(max(v_{q1}^{ref},\ -v_{max}), v_{max}) \\ v_{d1}^{sat} &= min(max(v_{d1}^{ref}, -v_{max}), v_{max2}) \end{aligned} \tag{5}$$

where,$v_{max2} = \sqrt{v_{max}^2 - {v_{q1}^{ref}}^2}$.

3) If dq-axis have equal priority, (6) is hold:

$$\begin{aligned} v_{d1}^{sat} &= min(max(v_{d1}^{ref},\ -nv_{d1}^{ref}), nv_{d1}^{ref}) \\ v_{q1}^{sat} &= \min(\max(v_{q1}^{ref}, -nv_{q1}^{ref}), nv_{q1}^{ref}) \end{aligned} \tag{6}$$

where, $n = \frac{v_{max}}{\sqrt{{v_{d1}^{ref}}^2 + {v_{q1}^{ref}}^2}}$.

III. Simulation Results

A simulation is built in Matlab/Simulink to compare proposed field weakening loop with different prioritization. Where, the current controller is chosen to be the complex vector current regulator as designed in [10]. A test is carried out in current control mode, where the machine speed is fixed to 20krpm, while the q-axis current reference steps up from 0 to 32 A at 0.03 s and steps down from 32 to 0 A at 0.08 s. 32A is selected since it provides the rated 50 kW output power. The current responses with different prioritization are compared in Fig.4. As shown, q-axis prioritization provides the most aggressive i_q (i.e. torque)

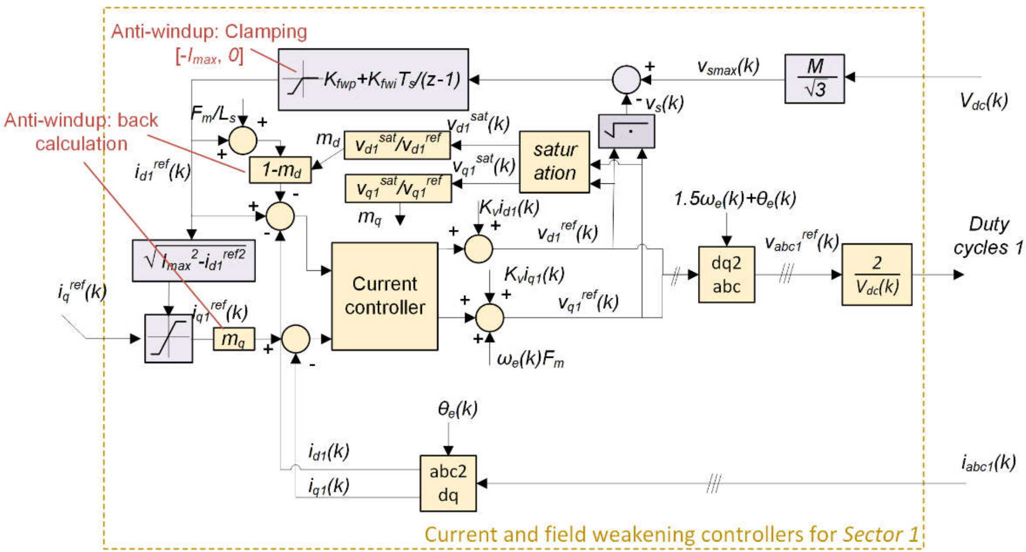

Fig.3 Proposed field weakening loop with anti-windup and saturation.

response, while d-axis prioritization provides the mildest torque response. Equal prioritization balances the torque response and voltage limitation.

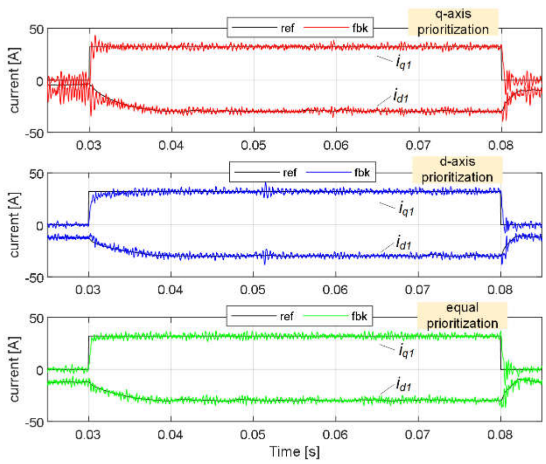

Fig.4 Step response of currents in field weakening.

IV.CONCLUSIONS

Field weakening control has increasing importance as the speed of the machine increases. A high speed nine-phase PMSM has been designed for MEA for the sake of higher power density and increased fault-tolerant capability. This paper demonstrates the design and tuning of a simple filed weakening loop without considering the anti-windup and saturations. And then, different anti-windup and saturation approaches are discussed and compared in the simulation. Guidelines on choosing the prioritization between torque control and voltage limitation will be given in the full paper.

ACKNOWLEDGMENT

This project has received funding from the Clean Sky 2 Joint Undertaking under the European Union’s Horizon 2020 research and innovation programme under grant agreement number 820913.

REFERENCES

[1] A. Recalde et al., "Energy Storage System Selection for Optimal Fuel Consumption of Aircraft Hybrid Electric Taxiing Systems," IEEE Trans. Transport Electrific, DOI: 10.1109/TTE.2020.3039759.

[2] X. Lang, T. Yang, H. B. Enalou, C. Li, S. Bozhko and P. Wheeler, “A dual-channel enhanced power generation architecture with backtoback converter for MEA Application,” IEEE Trans. Ind. Appl., vol. 56, no. 3, pp. 3006–3019, May/Jun. 2020.

[3] Aircraft Electric Power Characteristics, American Military Standard MILSTD-704F, Mar. 2004.

[4] Wai, J., and T. M. Jahns. "A new control technique for achieving wide constant power speed operation with an interior PM alternator machine." Industry Applications Conference. Vol. 2, 2001, pp. 807-814

[5] S. Bozhko, M. Rashed, C. I. Hill, S. S. Yeoh and T. Yang, "Flux-Weakening Control of Electric Starter–Generator Based on Permanent-Magnet Machine," IEEE Trans. Transport. Electrific., vol. 3, no. 4, pp. 864-877, Dec. 2017.

[6] Y. Chen, X. Huang, J. Wang and et.al, “Improved Flux-Weakening Control of IPMSMs Based on Torque Feedforward Technique,” IEEE Trans. Power Electron., pp. 1-1, 2018.

[7] Bon-Ho Bae, N. Patel, S. Schulz and Seung-Ki Sul, "New field weakening technique for high saliency interior permanent magnet motor," 38th IAS Annual Meeting on Conference Record of the Industry Applications Conference, 2003., Salt Lake City, UT, USA, 2003, pp. 898-905 vol.2.

[8] K. Åström, T. Hägglund, Advanced PID Control, ISA, Research Triangle Park, NC, August 2005.

[9] Yu-seok Jeong and Seung-Ki Sul, "Analysis and design of a decoupling current controller for AC machines: a unified transfer-matrix approach," Fourtieth IAS Annual Meeting. Conference Record of the 2005 Industry Applications Conference, 2005., Hong Kong, China, 2005, pp. 751-758 Vol. 1.

[10] M. Tang *et al.*, “Optimised current loop design for a high speed nine-phase permanent magnet synchronous machine in more electric aircraft: A case study,” *2021 IEEE Transp. Electrif. Conf. Expo, ITEC 2021*, pp. 665–671, 2021, doi: 10.1109/ITEC51675.2021.9490130.